Organophosphonate Functionalized Gd@C_{82} as a Magnetic Resonance Imaging Contrast Agent

Chun-Ying Shu,[†] Chun-Ru Wang,*[,†] Jian-Fei Zhang,[‡] Harry W. Gibson,[‡] Harry C. Dorn,[‡] Frank D. Corwin,[§] Panos P. Fatouros,[§] and T. John S. Dennis*[,△]

Institute of Chemistry, Chinese Academy of Sciences, Beijing 100080, China, Department of Chemistry, Virginia Polytechnic Institute and State University, Blacksburg, Virginia 24060, Department of Radiology, Virginia Commonwealth University, Richmond, Virginia 23298, and Centre for Materials Research, Queen Mary, University of London, London E1 4NS, U.K.

Received August 23, 2007. Revised Manuscript Received December 17, 2007. Accepted January 11, 2008

A new magnetic resonance imaging contrast agent containing organophosphonate functional groups was synthesized in high yield by a simple synthesis procedure. This molecule exhibits much higher longitudinal water proton relaxivity (37.0 mM^{-1} s^{-1}) than commercial Omniscan (Gd-DTPA BMA, 5.7 mM^{-1} s^{-1}) at 0.35 T. Notably, the relaxivity is larger than that of carboxylated Gd@C_{82} (16.0 mM^{-1} s^{-1}) under the same conditions, indicating that the functional groups have an important role on the image contrast enhancement. In addition, the introduction of phosphonate substituents may provide bone-targeting MRI contrast agents.

1. Introduction

Magnetic resonance imaging (MRI), one of the most powerful noninvasive methods in medicine, plays an important role in clinical diagnosis. Typically, the intrinsic contrast between tissues is augmented by the use of paramagnetic agents,[1] commonly the gadolinium(III) chelate compounds of DTPA, DO3A, and other similar linear and macrocyclic ligands, which efficiently decrease the spin–lattice relaxation time (T_1) of water protons, leading to brighter images and enhanced contrast between areas containing the contrast agent and the surrounding tissues.[2] However, the nontargeted biodistribution of the present MRI contrast agents and the limited chelate-site interaction with H_2O directly decrease the sensitivity in revealing anatomical details in vivo and detecting lesions for diagnosis. Furthermore, the clinical applications of many current macromolecular contrast agents (CAs) are limited because of potential toxicity of free Gd^{3+} ions released by the metabolism of the contrast agents[3] and high incidence of NSF in patients which receives high intravenous doses of Gd compounds. Therefore, further development of contrast agents with high efficiency and low toxicity are crucial for the early accurate diagnosis of pathological tissues.

Endohedral metallofullerenes[4] are fullerene-based species that incarcerate one or more metal atoms, which yields several potential medical applications: for example, antitumors,[5] radiotracers,[6] X-ray diffraction contrast agents,[7] and MRI contrast agents.[8] Indeed, water-soluble derivatives of Gd@C_{2n} ($2n = 60$, 82) and Gd_3N@C_{80} exhibit much higher relaxivities than commercial Magnevist (gadolinium-diethylenetriaminepentaacetic acid, Gd-DTPA) and Ominiscan as

* Corresponding authors. Tel. & Fax: (+86)10-62652120. E-mail: crwang@iccas.ac.cn (C.-R.W.); j.dennis@qmul.ac.uk (T.J.S.D.).
[†] Chinese Academy of Sciences.
[‡] Virginia Polytechnic Institute and State University.
[§] Virginia Commonwealth University.
[△] University of London.

(1) (a) Lauffer, R. B. *Chem. Rev.* **1987**, *87*, 901–927. (b) Caravan, P.; Ellison, J. J.; McMurry, T. J.; Lauffer, R. B. *Chem. Rev.* **1999**, *99*, 2293–2352. (c) Tóth, É. ; Merbach, A. E. Relaxivity of Gadolinium(III) complexes: Theory and Mechanism. In *The Chemistry of Contrast Agents in Medical Magnetic Resonance Imaging*; Merbach, A. E., Tóth, É., Eds.; Wiley: Chichester, U. K., 2001. (d) Brucher, E. *Top. Curr. Chem.* **2002**, *221*, 103–122.

(2) (a) Kadrmas, D. J.; Frey, E. C.; Tsui, B. M. W. *Phys. Med. Biol.* **1999**, *44*, 1843–1860. (b) Gabriel, M.; Hausler, F.; Bale, R.; Moncayo, R.; Decristoforo, C.; Kovacs, P.; Virgolini, I. *Eur. J. Nucl. Med. Mol. Imaging* **2005**, *32*, 1440–1451.

(3) (a) Rebizak, R.; Schaefer, M.; Dellacherie, E. *Bioconjugate Chem.* **1998**, *9*, 94–99. (b) Franano, F. N.; Edwards, W. B.; Welch, M. J.; Brechbiel, M. W.; Gansow, O. A.; Duncan, J. R. *Magn. Reson. Imaging* **1995**, *13*, 201–214.

(4) (a) Shinohara, H. *Rep. Prog. Phys.* **2000**, *63*, 843–862. (b) Nagase, S.; Kobayashi, K.; Akasaka, T. *Bull. Chem. Soc. Jpn.* **1996**, *69*, 2131–2142. (c) Fan, L. Z.; Yang, S. F.; Yang, S. H. *Fullerenes, Nanotubes, Carbon Nanostruct.* **2005**, *13*, 155–158.

(5) (a) Chen, C.; Xing, G. M.; Wang, J. X.; Zhao, Y. L.; Li, B.; Tang, J.; Jia, G.; Wang, T. C.; Sun, J.; Xing, L.; Yuan, H.; Gao, Y. X.; Meng, H.; Chen, Z.; Zhao, F.; Chai, Z. F.; Fang, X. H. *Nano Lett.* **2005**, *5*, 2050–2057. (b) Tabata, Y.; Murakami, Y.; Ikada, Y. *Jpn. J. Cancer Res.* **1997**, *88*, 1108–1116. (c) Tabata, Y.; Ikada, Y. *Pure Appl. Chem.* **1999**, *71*, 2047–2053.

(6) (a) Cagle, D. W.; Kennel, S. J.; Mirzadeh, S.; Alford, J. M.; Wilson, L. J. *Proc. Natl. Acad. Sci. U.S.A.* **1999**, *96*, 5182–5187. (b) Wilson, L. J.; Cagle, D. W.; Thrash, T. P.; Kennel, S. J.; Mirzadeh, S.; Alford, J. M.; Ehrhardt, G. J. *Coord. Chem. Rev.* **1999**, *190*, 199–207. (c) Thrash, T. P.; Cagle, D. W.; Alford, J. M.; Wright, K.; Ehrhardt, G. J.; Mirzadeh, S.; Wilson, L. J. *Chem. Phys. Lett.* **1999**, *308*, 329–336.

(7) (a) Lezzi, E. B.; Duchamp, J. C.; Fletcher, K. R.; Glass, T. E.; Dorn, H. C. *Nano Lett.* **2002**, *2*, 1187–1190. (b) Wharton, T.; Wilson, L. J. *Bioorg. Med. Chem.* **2002**, *10*, 3545–3554.

(8) (a) Zhang, S. R.; Sun, D. Y.; Li, X. Y.; Pei, F. K.; Liu, S. Y. *Fullerene Sci. Technol.* **1997**, *5*, 1635–1643. (b) Wilson, L. J. *The Electrochemical Society Interface* **1999**, (Winter), 24–28. (c) Mikawa, M.; Kato, H.; Okumura, M.; Narazaki, M.; Kanazawa, Y.; Miwa, N.; Shinohara, H. *Bioconjugate Chem.* **2001**, *12*, 510–514. (d) Kato, H.; Kanazawa, Y.; Okumura, M.; Taninaka, A.; Yokawa, T.; Shinohara, H. *J. Am. Chem. Soc.* **2003**, *125*, 4391–4397. (e) Bolskar, R. D.; Benedetto, A. F.; Husebo, L. O.; Price, R. E.; Jackson, E. F.; Wallace, S.; Wilson, L. J.; Alford, J. M. *J. Am. Chem. Soc.* **2003**, *125*, 5471–5478. (f) Lu, X.; Xu, J. X.; Shi, Z. J.; Sun, B. Y.; Gu, Z. N.; Liu, H. D.; Han, H. B. *Chem. J. Chin. Univ.* **2004**, *25*, 697–700. (g) Okumura, M.; Mikawa, M.; Yokawa, T.; Kanazawa, Y.; Kato, H.; Shinohara, H. *Academic Radiology* **2002**, *9*, S495–497. (h) Fatouros, P. P.; Corwin, F. D.; Chen, Z. J.; Broaddus, W. C.; Tatum, J. L.; Kettenmann, B.; Ge, Z.; Gibson, H. W.; Russ, J. L.; Leonard, A. P.; Duchamp, J. C.; Dorn, H. C. *Radiology* **2006**, *240*, 756–764.

10.1021/cm7023982 CCC: $40.75
Published on Web 02/21/2008

MRI contrast agents.[8] Most significantly, the fullerene cage is believed to hinder both chemical attack on the lanthanide ion and the escape of the lanthanide ion, which should effectively eliminate the toxicity of naked Gd^{3+}. Moreover, we may improve the biodistribution by modifying the cages with biologically active groups that exhibit high and specific affinity for a particular tissue, resulting in local contrast enhancement. Unfortunately, the metallofullerenes and modification have not yet found their way into clinical trials because of their complexity and relatively large size, and the latter in part governing the organ distribution.

Organic phosphonate compounds are biologically active species.[9] Owing to their high affinity to bone surfaces, organophosphonate have been widely used in medical treatment of bone disease[9c] during the last 20 years. At the same time, X-rays (bone fractures) and single photon emission computed tomography (SPECT) (99m Tc) imaging (bone diseases) are already excellent imaging modalities for bone. However, X-rays are providing only structural (anatomical) information on the basis of differential X-ray attenuation between bone and soft tissue. MRI as one of the most powerful noninvasive methods in medicine plays an important role in clinical diagnosis. Most importantly, it can provide high specificity and sensitivity for the detection of bone diseases due to the functionalized nature and high relaxivity of contrast agents. More recently, MRI contrast agents with phosphonates and bis(phosphonates) as targeting groups have been developed.[10] Unfortunately, the Gd(III) complexes are relatively unstable in vivo, which has hampered their applications.[11] In particular, the phosphonate groups strongly interact with the surface of hydroxyapatite, which weakens the binding of the Gd(III) ion, resulting in a decrease in stability of these complexes.[11b] Mirakyan and Wilson[12] reported a functionalized C_{60} with diphosphonate groups as a model system for the design and study of bone-vectored material.

Herein, we successfully introduced organophosphate groups to Gd@C_{82} by a Bingel reaction in a high yield, and the product was isolated by simple size-exclusion gel columns. In vitro water proton relaxivity confirmed its high efficiency as an MRI contrast agent.

2. Experimental Section

Fourier transform infrared (FTIR) spectroscopy measurements were performed using a Nicolet magna-IR750 spectrometer. X-ray photoelectron spectroscopy (XPS) measurements were taken with an ESCALab220i-XL electron spectrometer (VG Scientific) using 300W Al Kα radiation. The mass spectral data was collected by matrix-assisted laser desorption/ionization−time-of-flight (MALDI-TOF) mass spectrometry using the Biflex II spectrometer (Bruker, Germany) and 4-hydroxyl-α-cyano cinnamic acid as the matrix. The in vitro MRI phantom studies were performed at a 4 μM Gd by the T_1-weighted spin–echo method at a 1.5 T clinical MR instrument (Sonata Siemens). The concentration of Gd in the aqueous solutions was determined by inductively coupled plasma atomic emission spectroscopy (ICP-AES, Leeman, U.S.A.) at 342.247 nm. The relaxation times were measured at three different magnetic field strengths: 0.35 T with a TEACH SPIN PS1-B instrument, 2.4 T with a Bruker/Biospec, and 9.4 T with a Varian Inova 400. The inversion–recovery method was used to measure T_1, and the Carr−Pucell−Meiboom−Gill method was used for measurement of T_2. In that, the inversion times were set from 0.25 to 3 s, and various inversion and echo times (at least 5 times per concentration) were used for the measurement of T_1 and T_2. The relaxivities (r_1 and r_2 in $mM^{-1}\ s^{-1}$) in aqueous solution (pH = 7) were obtained from linear least-squares determination of the slopes of relaxation rates ($1/T_1$ and $1/T_2$) versus [Gd] plots. Dynamic light scattering (DLS) measurements were carried out with a Malvern Instrument (Zetasizer/nano Series, model ZEN3600).

Scheme 1. Functionalization Reaction of Gd@C_{82}

$$Gd@C_{82}+CH_2(PO_3Et_2)_2 \xrightarrow[\text{ii } H_2O]{\text{i NaH / Toluene}} Gd@C_{82}O_m(OH)_n(C(PO_3Et_2)_2)_l$$

The Gd@C_{82} was synthesized by a modified Krätschmer−Huffman method and isolated by multistage HPLC technique.[13] The organophosphonate-containing water-soluble derivative of Gd@C_{82} (Gd@$C_{82}O_2(OH)_{16}(C(PO_3Et_2)_2)_{10}$, abbreviated as TEMDP-EMF), was synthesized by a Bingel method.[14] NaH (1 g) was added to a solution of Gd@C_{82} (ca. 5 mg) and tetraethyl methylenediphosphonate (10 μL) in dry toluene (25 mL) at room temperature. After stirring for 1 h, deionized water (50 mL) was added dropwise, and the resulting solution was stirred at room temperature for additional 24 h; the organic layer became colorless (Scheme 1).

The brown aqueous layer was then separated from the colorless organic layer and concentrated. This residue was purified on a Sephadex G-25 (Pharmacia) size-exclusion gel column with distilled water as eluent. The brown fraction (pH = 6−7) was concentrated in vacuum. The overall reaction yield was more than 80%. The molecular composition was determined by MALDI-TOF mass spectrum, FTIR, and XPS.

3. Results and Discussion

Similar to other water-soluble fullerenols[15] and endohedral fullerenols, such as Pr@$C_{82}(OH)_n$,[16] the MALDI-TOF MS of the TEMDP-EMFs exhibited only a strong Gd@C_{82} ionic peak (Figure 1) while no parent ion peak was observed. It is well-known that the laser desorption process easily strips off functional groups from such endohedral fullerenes.[15b,16] Because Gd@C_{82} is completely insoluble in water, the observation of strong Gd@C_{82} ionic signals in water-soluble

(9) (a) Cheng, F.; Yang, X.; Fan, C.; Zhu, H. *Tetrahedron* **2001**, *57*, 7331–7335. (b) Kubíček, V.; Rudovsky, J.; Kotek, J.; Hermann, P.; Elst, L. V.; Muller, R. N.; Kolar, Z. I.; Wolterbeek, H. T.; Peters, J. A.; Lukes, I. *J. Am. Chem. Soc.* **2005**, *127*, 16477–16485. (c) Fleisch, H. *Bisphosphonates in Bone Disease*, 4th ed.; Academic Press: London, 2000.

(10) (a) Adzamli, I. K.; Gries, H.; Johnson, D.; Blau, M. *J. Med. Chem.* **1989**, *32*, 139–144. (b) Adzamli, I. K.; Johnson, D.; Blau, M. *Invest. Radiol.* **1991**, *26*, 143–148. (c) Adzamli, I. K.; Blau, M.; Pfeffer, M. A.; Davis, M. A. *Magn. Reson. Med.* **1993**, *29*, 505–511. (d) Greb, W.; Blum, H.; Roth, M. PCT WO2003/097074. *Chem. Abstr.* **2003**, 931193.

(11) (a) Adzamli, I. K.; Blau, M. *Magn. Reson. Med.* **1991**, *17*, 141–148. (b) Bligh, S. W. A.; Harding, C. T.; McEwen, A. B.; Sadler, P. J.; Kelly, J. D.; Marriott, J. A. *Polyhedron* **1994**, *13*, 1937–1943.

(12) Mirakyan, A. L.; Wilson, L. J. *J. Chem. Soc., Perkin Trans.* **2002**, *2*, 1173–1176.

(13) Huang, H. J.; Yang, S. H. *J. Phys. Chem. B* **1998**, *102*, 10196–10200.

(14) Yin, J.-J.; Li, Y.-G.; Li, B.; Li, W.-X.; Jin, L.-M.; Zhou, J.-M.; Chen, Q.-Y. *Chem. Commun.* **2005**, 3041–3043.

(15) (a) Kato, H.; Suenaga, K.; Mikawa, W.; Okumura, M.; Miwa, N.; Yashiro, A.; Fujimura, H.; Mizuno, A.; Nishida, Y.; Kobayashi, K.; Shinohara, H. *Chem. Phys. Lett.* **2000**, *324*, 255–259. (b) Sun, D. Y.; Liu, Z. Y.; Guo, X. H.; Liu, S. Y. *Rapid Commun. Mass Spectrom.* **1997**, *11*, 114–116.

(16) Sun, D. Y.; Huang, H. J.; Yang, S. H.; Liu, Z. Y.; Liu, S. Y. *Chem. Mater.* **1999**, *11*, 1003–1006.

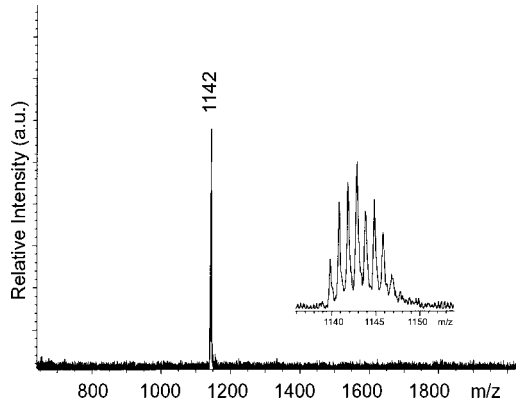

Figure 1. Negative-ion MALDI-TOF MS of water-soluble phosphonate derivative of Gd@C_{82} (TEMDP-EMF).

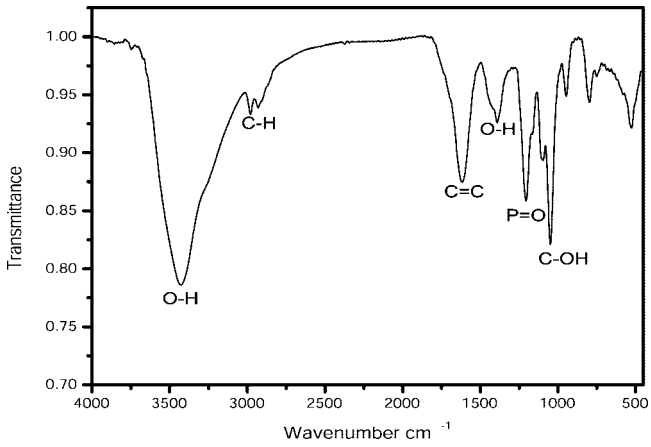

Figure 2. FTIR spectrum of the water-soluble phosphonate derivative of Gd@C_{82} (TEMDP-EMF).

samples indicates the existence of intact endohedral fullerene cages, which is consistent with modification of Gd@C_{82} to a water-soluble derivative. The FTIR spectrum (Figure 2) exhibits a broad and strong peak centered at 3427 cm^{-1} which is assigned to the O—H stretching vibration, whereas the weak peaks at approximately 2979 and 2930 cm^{-1} are assigned to C—H stretching vibration. The several low-lying sharp characteristic peaks at 1616, 1392, 1205, and 1048 cm^{-1} are assigned to the C═C stretching, O—H deformation, P═O stretching, and C—OH stretching vibrations, respectively. The weak peak at 527 cm^{-1} is ascribed to skeletal vibration of the C_{82} cage, revealing the existence of hydroxyl and phosphonate functional groups.

The UV–vis−NIR absorption spectra of TEMDP-EMFs and Gd@C_{82} (Figure 3) were measured in water and toluene, respectively. The spectra revealed that the Gd@C_{82} derivatives lost most of the characteristic absorbance of Gd@C_{82} at 635 and 969 nm, implying that the electronic structure of Gd@C_{82} is changed after introducing hydroxyl and tetraethyl methylenediphosphonate groups on the carbon cage.

The XPS spectrum of as-synthesized TEMDP-EMFs film yields elemental peaks from C 1s, O 1s, and P 2p. Similar to other water-soluble derivatives of endohedral fullerenes,[16,17] peaks corresponding to metal (Gd $3d_{3/2}$, Gd $3d_{5/2}$) were also

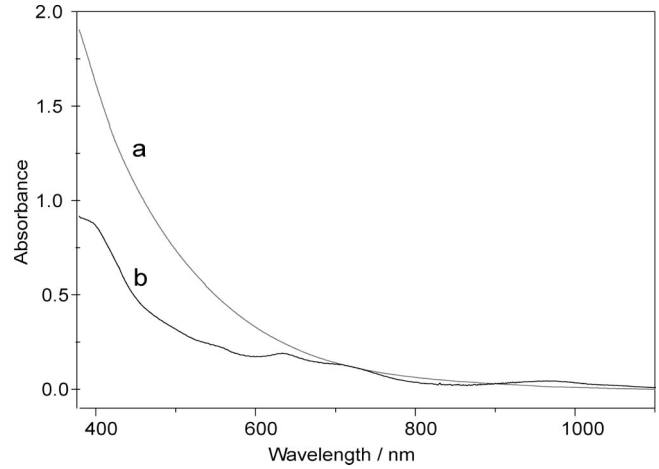

Figure 3. UV–vis−NIR absorption spectra of (a) TEMDP-EMF in water and (b) Gd@C_{82} in toluene.

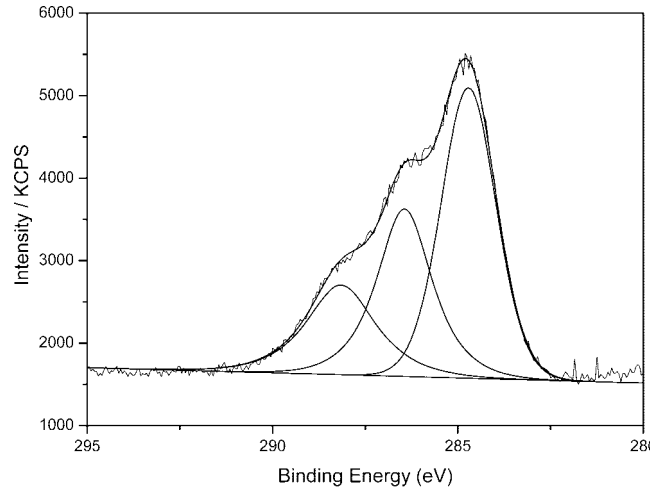

Figure 4. XPS spectrum of C 1s in TEMDP-EMF.

observed. However, the low signal-to-noise ratio of the XPS data prohibited a detailed analysis. Considering the C:O:P atomic ratio and the relative contents of different chemical states for carbon (Figure 4), oxygen, and phosphorus elements, we can estimate the average number of hydroxyl, phosphonate ester, hemiketal (RO−C−OH) and carbonyl groups. Thus, the molecular formula of the TEMDP-endohedral fullerene is Gd@$C_{82}O_2(OH)_{16}(C(PO_3Et_2)_2)_{10}$. It is well-known that the reaction products for a fullerenol material prepared by this method are very complex.[18] The uncertainty in structure and the paramagnetic property of gadolinium restrict the detailed analysis by NMR.

To explore the potential of our molecule as an MRI contrast agent, the proton relaxivity,[1b] the r_1 value (the paramagnetic longitudinal relaxation rate enhancement of water protons, referenced to 1 mM concentration) is used along with transverse relaxivity, r_2.

The r_1/r_2 (mM^{-1} s^{-1}/mM^{-1} s^{-1}) values at different magnetic fields are 37.0/42.0 (0.35 T), 38.9/68.3 (2.4 T), and 19.9/73.7 (9.4T), respectively. Notably, the r_1 of TEMDP-EMF at 0.35 T and 25 °C is more than an order of magnitude

(17) Shu, C. Y.; Gan, L. H.; Wang, C. R.; Pei, X. L.; Han, H. B. *Carbon* **2006**, *44*, 496–500.

(18) Husebo, L. O.; Sitharaman, B.; Furukawa, K.; Kato, T.; Wilson, L. J. *J. Am. Chem. Soc.* **2004**, *126*, 12055–12064.

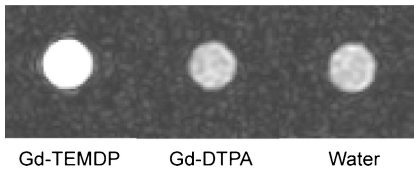

Figure 5. T_1-weighted MRI of Gd@$C_{82}O_2(OH)_{16}(C(PO_3Et_2)_2)_{10}$(Gd-TEMDP), Gd-DTPA, and water phantoms at the Gd concentration of 4 μM by 1.5 T spin–echo method with T_R/T_E = 800/15 ms, FOV = 17.1 × 22.8 cm^2 at 24 °C.

higher than that of commercial Omniscan (Gd-DTPA BMA, 5.7 mM^{-1} s^{-1}) under the same conditions. Interestingly, the relaxivity is higher than that of our earlier synthesized Gd@$C_{82}O_6(OH)_{16}(NHCH_2CH_2COOH)_8$[22] (16.0 mM^{-1} s^{-1} at 0.35 T and 25 °C), revealing that the functional groups can tune the water proton relaxivity. The in vitro MRI of phantoms at a 4 μM Gd obtained by the T_1-weighted spin–echo method reveal that the MRI signal-enhancing efficiency of TEMDP-EMF is also far higher than that of Gd-DTPA (Figure 5), which is consistent with the above proton relaxivity analysis of the two contrast agents.

In gadofullerene-based MRI contrast agents, water molecules are not directly coordinated to the metal ion, so the present spin relaxation belongs to the so-called "second sphere mechanism".[1a] Besides the electron transfer between metal and carbon cage, the large reorientational motion of functionalized metallofullerenes and large number of surrounding water molecules are expected to play crucial roles in the high relaxivity.[19]

So far, only three types of functionalized MRI contrast agents based on Gd@C_{2n} ($2n$ = 60, 82) were reported. One is the polyhydroxylated metallofullerenes;[8a–d] the others are carboxylate[8e,17] and sulfonate substituted metallofullerenes.[8f] Notably, polyhydroxylated metallofullerenes with high reticuloendothelial system (RES) uptake exhibited much higher relaxivity than the sulfonated system, which exhibits a favorable non-RES distribution. A series of studies[19–23] indicated that besides the number of hydroxyl groups, aggregating size and distance of interaction between carbon cage and water molecules play predominant roles in proton relaxivity. That is, polyhydroxylated metallofullerenes with larger aggregation sizes and shorter interaction distances exhibit much higher relaxivity than carboxylated metallofullerenes under the same conditions. Recently, Fatouros et al.[8h] reported an MRI contrast agent based on a trimetallic nitride templated metallofullerene (TNT EMF), $Gd_3N@C_{80}$, which was PEGylated and hydroxylated. This compound exhibited the highest relaxivity reported so far. Besides the fast water exchange rate, the cocontribution of three paramagnetic Gd(III) ions in one carbon cage together with the slow rotational time caused by the attachment of a large substituent, dipoly(ethylene glycol) malonate, plays a crucial role. In contrast, our synthesized organophosphonate functionalized metallofullerene with 16 hydroxyl and 10 organophosphonate groups attached on the carbon cage also exhibit much higher relaxivity than carboxylated metallofullerenes, which possess the same number of hydroxyl and another eight carboxyl groups.[17] This may be ascribed to organophosphonate functional groups. DLS experiments confirms our conclusion. Figure 6 displays the hydrodynamic diameter distribution of as-synthesized Gd@$C_{82}O_2(OH)_{16}(C(PO_3Et_2)_2)_{10}$ in water. The data clearly display bimodal distributions for the compound, which is similar to that of Gd@$C_{60}(OH)_x$ and Gd@$C_{60}[C(COOH)_2]_{10}$[21] but different from that of our formerly synthesized Gd@$C_{82}O_6(OH)_{16}(NHCH_2CH_2COOH)_8$,[22] since the latter displayed a unimodal distribution. Laus et al.[20] reported that phosphate can disrupt the aggregation of Gd@$C_{60}(OH)_x$ and Gd@$C_{60}[C(COOH)_2]_{10}$ by intercalation of $H_2PO_4^-$ and HPO_4^{2-} ions into the hydrogen-bond network around the malonate or hydroxyl groups of the gadofullerenes. On the contrary, in our compound, Gd@$C_{82}O_2(OH)_{16}(C(PO_3Et_2)_2)_{10}$, the organophosphonate can merge the molecules together via strong hydrogen bonds, resulting in larger and slower tumbling entities and correspondingly higher relaxivity relative to carboxylated gadofullerenes. This was verified by the bimodal distributions with average hydrodynamic diameter at 55 and 300 nm, respectively.

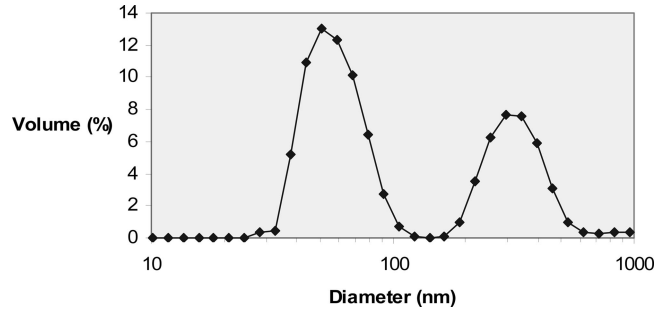

Figure 6. Size distributions of Gd@$C_{82}O_2(OH)_{16}(C(PO_3Et_2)_2)_{10}$ (Gd-TEMDP) in water at room temperature.

4. Conclusions

We synthesized a novel MRI contrast agent containing organophosphonate functionalized groups in high yield by a simple procedure. This molecule exhibits much higher water proton relaxivity than commercial Gd-DTPA and carboxylated Gd@C_{82} reported. We postulate that in addition to an effective number of hydroxyl groups, the phosphonate groups on the carbon cage are important in affecting the relaxivity. The introduction of phosphonate substituents may also provide great potential of this new compound as bone-targeting MRI contrast agents.

Acknowledgment. C.-R.W. thanks NSFC (Nos. 50225206, 90206045, 20121301), the Major State Basic Research Program of China "Fundamental Investigation on Micro-Nano Sensors and Systems based on BNI Fusion" (Grant 2006CB300402). T.J.S.D. thanks the Royal Society for an Incoming Short Visit−China with C.-R.W.

CM7023982

(19) Toth, E.; Bolskar, R. D.; Borel, A.; Gonzalez, G.; Helm, L.; Merbach, A. E.; Sitharaman, B.; Wilson, L. J. *J. Am. Chem. Soc.* **2005**, *127*, 799–805.
(20) Laus, S.; Sitharaman, B.; Toth, V.; Bolskar, R. D.; Helm, L.; Asokan, S.; Wong, M. S.; Wilson, L. J.; Merbach, A. E. *J. Am. Chem. Soc.* **2005**, *127*, 9368–9369.
(21) Sitharaman, B.; Bolskar, R. D.; Rusakova, I.; Wilson, L. J. *Nano Lett.* **2004**, *4*, 2373–2378.
(22) Shu, C. Y.; Zhang, E. Y.; Xiang, J. F.; Zhu, C. F.; Wang, C. R.; Pei, X. L.; Han, H. B. *J. Phys. Chem. B* **2006**, *110*, 15597–15601.
(23) Laus, S.; Sitharaman, B.; Toth, E.; Bolskar, R. D.; Helm, L.; Wilson, L. J.; Merbach, A. E. *J. Phys. Chem. C* **2007**, *111*, 5633–5639.